

How to measure the mass of the W

Matthew H. Austern

Lawrence Berkeley Laboratory, University of California, Berkeley, California, 94720

and

Physics Department, University of California at Berkeley, Berkeley, California, 94720

Robert N. Cahn

Lawrence Berkeley Laboratory, University of California, Berkeley, California, 94720

(February 26, 2019)

Abstract

We perform a numerical calculation of the total cross section $\sigma(e^+e^- \rightarrow W^+W^-)$ as a function of energy, taking into account the finite width of the W and the most important radiative corrections. We present these results, in tabular form, for several values of M_W . Using these results, we investigate running strategies for integrated luminosities that might be available at LEP 200 and estimate the accuracy to which it will be possible to determine the mass of the W by measuring this cross section near threshold. With an integrated luminosity of 100 pb^{-1} it should be possible to achieve a precision of 100 MeV, and with an integrated luminosity of 500 pb^{-1} , a precision of 60 MeV.

PACS numbers: 14.80.Er, 13.38.+c, 13.10.+q

I. INTRODUCTION

The gauge sector of the Standard Model of electroweak physics is described by three parameters, which can be chosen to be α , the electromagnetic coupling constant, and M_Z and M_W , the masses of the weak gauge bosons. Of these three, M_W is by far the least well known. A more practical choice of parameters is α , M_Z , and G_F , where $G_F = (1.16639 \pm 0.00002) \times 10^{-5} \text{ GeV}^{-2}$ is the Fermi decay constant. The mass of the W , then, can be predicted in terms of these three parameters; this prediction depends on some additional physics as well, most notably the masses of the top quark and the Higgs boson. Despite this dependence, and despite the large uncertainty in the measured value of M_W , a comparison of M_W to the predicted value is already a stringent test of the Standard Model.

The W mass is currently measured [1] to be $80.22 \pm 0.26 \text{ GeV}$, where this value is obtained by direct reconstruction of W events at $\bar{p}p$ colliders; it is expected [2] that future experiments at the Fermilab Tevatron will be able to reduce this uncertainty to less than 150 MeV. This is still, however, a much larger relative uncertainty than in the other fundamental parameters of the Standard Model.

One of the major motivations for upgrading LEP to an energy of $\sqrt{s} \approx 200 \text{ GeV}$ is to measure M_W more precisely. Several methods have been proposed, including measurement of the end point of the leptonic decay spectrum, direct reconstruction of the invariant mass of the W 's decay products [3], and measurement of the threshold for W^+W^- pair production. We will discuss the last of these methods.

In principle, M_W can be measured simply by determining the end point of the W^+W^- spectrum; in practice, however, there is no sharp end point, since the W has a finite width, with $\Gamma_W = 2.12 \pm 0.11 \text{ GeV}$. Initial-state radiation results in a further smearing of the cross section. In the regime $\sqrt{s} \approx 2M_W$, which we will call the threshold region, the cross section rises steeply as a function of energy, varying from about 2 pb at $\sqrt{s} = 160 \text{ GeV}$ to 4 pb at $\sqrt{s} = 162 \text{ GeV}$. A precise measurement of the cross section in this region provides essentially the same information as would be obtained from determination of the end point, if a sharp end point existed.

Once the finite W width and initial-state radiation are taken into account, there is no simple analytic form for the W^+W^- production cross section. Accordingly, we have calculated this cross section numerically, and used these results to estimate the precision to which it will be possible to measure M_W at LEP 200.

II. CALCULATION OF THE W PAIR PRODUCTION CROSS SECTION

At tree level, W^+W^- production at an e^+e^- collider proceeds by the diagrams in Fig. 1. Evaluation of these diagrams is straightforward; unfortunately, if done naively, it yields an unrealistic answer near threshold. The W decays rapidly, and it is incorrect to put it on-shell in the final state.

A more realistic answer [4] is given by

$$\sigma(s) = \int_0^s dm_1^2 \rho(m_1^2) \int_0^{(\sqrt{s}-m_1)^2} dm_2^2 \rho(m_2^2) \sigma_0(s, m_1, m_2), \quad (1)$$

where σ_0 is the cross section for production of two off-shell W 's with masses m_1 and m_2 , and where ρ is a weight factor,

$$\rho(m^2) = \frac{1}{\pi} \frac{\Gamma_W}{M_W} \frac{m^2}{(m^2 - M_W^2)^2 + m^4 \Gamma_W^2 / M_W^2}. \quad (2)$$

This expression for ρ differs slightly from that given in Ref. [4], but the difference is numerically inconsequential. A derivation is given in the Appendix.

The cross section for pair-production of off-shell W 's has been calculated by Muta, Najima, and Wakaizumi [4], and their result is

$$\sigma_0(s, m_1, m_2) = \frac{1}{32\pi s^2 m_1^2 m_2^2} (a_{\gamma\gamma} + a_{ZZ} + a_{\gamma Z} + a_{\nu\nu} + a_{\nu Z} + a_{\nu\gamma}), \quad (3)$$

where

$$a_{\gamma\gamma} = \frac{e^4}{s^2} G_1(s, m_1, m_2), \quad (4a)$$

$$a_{ZZ} = \frac{g^4 (1 - 4 \sin^2 \theta_W)^2 + 1}{16 (s - M_Z^2)^2 + M_Z^2 \Gamma_Z^2} G_1(s, m_1, m_2), \quad (4b)$$

$$a_{\gamma Z} = \frac{e^2 g^2 (1 - 4 \sin^2 \theta_W)}{2} \frac{s - M_Z^2}{s (s - M_Z^2)^2 + M_Z^2 \Gamma_Z^2} G_1(s, m_1, m_2), \quad (4c)$$

$$a_{\nu\nu} = \frac{g^4}{8} G_2(s, m_1, m_2), \quad (4d)$$

$$a_{\nu Z} = \frac{g^4}{8} (2 - 4 \sin^2 \theta_W) \frac{s - M_Z^2}{(s - M_Z^2)^2 + M_Z^2 \Gamma_Z^2} G_3(s, m_1, m_2), \quad (4e)$$

$$a_{\nu\gamma} = \frac{e^2 g^2}{2} \frac{1}{s} G_3(s, m_1, m_2), \quad (4f)$$

$$G_1 = \lambda^{3/2} \left[\frac{\lambda}{6} + 2(s(m_1^2 + m_2^2) + m_1^2 m_2^2) \right], \quad (5a)$$

$$G_2 = \lambda^{1/2} \left[\frac{\lambda}{6} + 2(s(m_1^2 + m_2^2) - 4m_1^2 m_2^2) \right] + 4m_1^2 m_2^2 (s - m_1^2 - m_2^2) F, \quad (5b)$$

$$G_3 = -\lambda^{1/2} \left[\frac{\lambda}{6} (s + 11m_1^2 + 11m_2^2) + 2s(m_1^4 + 3m_1^2 m_2^2 + s_2^4) - 2(m_1^6 + m_2^6) \right] + 4m_1^2 m_2^2 (s(m_1^2 + m_2^2) + m_1^2 m_2^2) F, \quad (5c)$$

$$\lambda = s^2 + m_1^4 + m_2^4 - 2(sm_1^2 + sm_2^2 + m_1^2 m_2^2), \quad (6)$$

and

$$F = \ln \left(\frac{s - m_1^2 - m_2^2 - \sqrt{\lambda}}{s - m_1^2 - m_2^2 + \sqrt{\lambda}} \right). \quad (7)$$

When both W 's are on-shell, *i.e.*, $m_1 = m_2 = M_W$, this reduces to the well-known form [5]

$$\begin{aligned}
\sigma(s) = \frac{\pi\alpha^2\beta}{2s\sin^4\theta_W} & \left[\left(1 + 2\frac{M_W^2}{s} + 2\frac{M_W^4}{s^2}\right) \frac{L}{\beta} - \frac{5}{4} \right. \\
& + \frac{M_Z^2(1 - 2\sin^2\theta_W)}{s - M_Z^2} \left(2\frac{M_W^4}{s^2} \left(1 + 2\frac{s}{M_W^2}\right) \frac{L}{\beta} - \frac{1}{12} \frac{s}{M_W^2} - \frac{5}{3} - \frac{M_W^2}{s} \right) \\
& \left. + \frac{M_Z^4(1 - 2\sin^2\theta_W)^2}{48(s - M_Z^2)^2} \beta^2 \left(\frac{s^2}{M_W^4} + 20\frac{s}{M_W^2} + 12 \right) \right], \tag{8}
\end{aligned}$$

where β is the speed of the W 's in the center of mass frame and

$$L = \ln \frac{1 + \beta}{1 - \beta}. \tag{9}$$

Numerical evaluation of Eq. 1 is somewhat time-consuming, since it involves two nested integrals, both of which are over sharp peaks. Fortunately, it is possible to make a vastly simplifying approximation:

$$\sigma(s) \approx \int_0^{(\sqrt{s}-M_W)^2} dm^2 \tilde{\rho}(m^2) \sigma_0(s, m, M_W), \tag{10}$$

where the weight factor $\tilde{\rho}$ is exactly the same as the weight factor ρ defined in Eq. (2), except that the W width, Γ_W , is replaced by $2\Gamma_W$.

Fig. 2 compares the cross section given by Eq. (1) to that given by Eq. (10). The approximation of Eq. (10), of course, breaks down completely near $\sqrt{s} \lesssim M_W$. This, however, is not the domain of interest, and in the region near threshold, $\sqrt{s} \approx 2M_W$, the approximation is excellent.

Several other higher-order effects are also significant. The most important are the running values of the gauge coupling constants, and initial-state radiation. The first of these can be taken into account simply by using the values for the coupling constants renormalized at a scale near M_W ; we use the values measured [6] at M_Z . Inclusion of initial-state radiation requires additional work.

Although initial-state radiation is a purely electromagnetic effect, and is thus suppressed by a factor of α , it is nonetheless significant because it is enhanced by a factor of $\ln(M_W^2/m_e^2)$, representing the presence of two very different energy scales. Using the formalism of Kuraev and Fadin [7], it is possible to sum all orders of initial-state radiation by performing a single integral:

$$\sigma(s) = t \int_0^{\sqrt{s}/2} dk \left[\frac{1}{k} \left(1 + \frac{3t}{4}\right) \left(\frac{2k}{\sqrt{s}}\right)^t - \frac{2}{\sqrt{s}} \left(1 - \frac{k}{\sqrt{s}}\right) \right] \sigma_0 \left[(\sqrt{s} - k)^2 \right], \tag{11}$$

where

$$t = \frac{2\alpha}{\pi} \left(\ln \left(\frac{M_W^2}{m_e^2} \right) - 1 \right) \approx 0.1065. \tag{12}$$

The second term in the integral represents single-photon hard bremsstrahlung, while the first is the result of summing all orders of soft photon emission. This formalism has previously been used to include the effects of initial-state radiation to all orders in the calculation

of $\sigma(e^+e^-) \rightarrow Z$ [8]. The difference between this result and the $\mathcal{O}(\alpha)$ calculation can be substantial.

Several groups [9] have performed full one-loop calculations of $\sigma(e^+e^- \rightarrow W^+W^-)$. Our calculation is considerably simpler, but contains most of the relevant physics, including initial-state radiation beyond leading order in α .

Fig. 3 shows the results of including initial-state radiation in the calculation of $\sigma(e^+e^- \rightarrow W^+W^-)$. Note that initial-state radiation makes a contribution roughly equal in magnitude to that of the W 's width, and that it has the effect of making the threshold for W pair production even less sharp.

Although there is no longer a sharp threshold, $\sigma(e^+e^- \rightarrow W^+W^-)$ still depends strongly on the value of the W mass; as shown in Fig. 4, this dependence is strongest for $E \approx M_W$. It is possible, then, to measure M_W by studying the threshold behavior of $\sigma(W^+W^-)$. Table I presents the same information, for masses within two standard deviations of the current central value, in tabular form.

Note that the behavior of σ in the threshold region is mainly due to kinematic effects [10], so it is proper to use it for a determination of M_W . The behavior of the cross section near the peak, at around $\sqrt{s} \approx 220$ GeV, is also of interest, but for different reasons. At this point, the total cross section depends on delicate gauge cancellations, so it is a sensitive probe of the Standard Model gauge structure.

III. MEASUREMENT OF M_W AT LEP 200

A. Lower bound on the statistical error

The most favorable situation possible would be if there were no uncertainty in the luminosity or the energy of the beam, and if there were no theoretical uncertainties; in this case, as seen in Fig. 4, measurement of the cross section at even a single point could determine M_W , and the error in M_W would be purely statistical.

The error in the measured value of M_W is given by

$$\delta M = \left| \frac{d\sigma}{dM} \right|^{-1} \delta\sigma, \quad (13)$$

and, if the error is assumed to be purely statistical,

$$\delta\sigma = \frac{\delta N}{\mathcal{I}}, \quad (14)$$

where $\mathcal{I} = \int d\mathcal{L}$ is the integrated luminosity and δN is the statistical error in the number of W^+W^- events observed. For $N \gg 1$ the statistical error approaches \sqrt{N} , and

$$\delta\sigma = \sqrt{\frac{\sigma}{\mathcal{I}}}. \quad (15)$$

The quantity $d\sigma/dM$ can be read off from Table I, but there is a simpler way to obtain a rough estimate. Near threshold, as seen in Fig. 4, the most important effect of changing M_W is simply a shift in the W^+W^- spectrum, *i.e.*,

$$\sigma(E, M_W + \delta M) \approx \sigma(E - \delta M, M_W), \quad (16)$$

where $E = \sqrt{s}/2$. Roughly, then,

$$\left| \frac{\partial \sigma}{\partial M} \right| \approx \left| \frac{\partial \sigma}{\partial E} \right|, \quad (17)$$

and, measuring the cross section at some particular value of E , the error in M_W is given by

$$\delta M_W \approx \sqrt{\sigma} \left| \frac{\partial \sigma}{\partial E} \right|^{-1} \frac{1}{\sqrt{\mathcal{I}}}. \quad (18)$$

Independent of \mathcal{I} , then, the optimum energy at which to make this measurement is where $|\partial\sigma/\partial E|/\sqrt{\sigma}$ is maximized; this is at $E \approx M_W$. The precision that may be attained is roughly

$$\delta M_W \approx \frac{870 \text{ MeV}/\text{pb}^{1/2}}{\sqrt{\mathcal{I}}}. \quad (19)$$

With an integrated luminosity of 1000 pb^{-1} , this would mean $\delta M_W \approx 30 \text{ MeV}$, which is comparable to the precision to which M_Z is known.

As a rough guide to systematic errors, we note that if the measured value of σ depends multiplicatively on some parameter C , then

$$\delta M_W = \sigma \left| \frac{\partial \sigma}{\partial M} \right|^{-1} \frac{\delta C}{C}. \quad (20)$$

For example, the measured cross section depends multiplicatively on the detector efficiency, and on the luminosity. Certain sources of theoretical error can also, at least approximately, be represented this way. Using the values found in Table I, we can rewrite this relation as

$$\delta M_W \approx 1.7 \text{ GeV} \frac{\delta C}{C}. \quad (21)$$

B. Theoretical error

There are three potential sources of theoretical error in this measurement: Model dependence, uncertainty in the input parameters, and incomplete inclusion of radiative corrections.

In general, $\sigma(e^+e^- \rightarrow W^+W^-)$ is model dependent: The calculation we have presented assumes the minimal Standard Model, and it will be changed if additional physics beyond this framework is included. This effect, however, is most severe far above threshold, where delicate gauge cancellations are necessary to preserve unitarity. Near threshold, the behavior of the cross section is mainly determined by kinematics, and is less sensitive to the inclusion of additional physics. For $\sqrt{s} \approx 160 \text{ GeV}$, model dependence is a negligible source of theoretical error.

Uncertainty in the input parameters is also a negligible source of error. The input parameters used in calculating the W^+W^- cross section are the electroweak coupling constants,

which, in turn, can be calculated in terms of α , G_F , and M_Z . The least well known of these, M_Z , is still known to better than 0.1%, so this error is also negligible.

The cross section given in Table I is fundamentally a tree-level calculation. We have included initial-state radiation, the running of the gauge coupling constants, and the imaginary part of the W 's vacuum polarization, but we have neglected several other one-loop effects; the dominant such effect is probably the vacuum polarization of the photon and the Z . By analogy with physics at the Z peak, we expect that these corrections are less than 1%. Similarly, we expect that the approximations used in deriving Eq. (11) are of this order. In the threshold region, the approximation of Eq. (10) is better than 1%, and we neglect it compared to other sources of error.

We will assume, then, that the theoretical error takes the form of an error in the overall normalization, and that it is approximately 1.5%. As discussed in Section III A, this corresponds to a systematic error in M_W of approximately 20 MeV.

C. Systematic error

One important source of systematic error is the width of the W , Γ_W . In principle, it would be possible to determine both Γ_W and M_W simultaneously, in the fit to $\sigma(s)$. This is, however, impractical. As shown in Fig. 5, the shape of the W^+W^- cross section is not very sensitive to Γ_W , particularly in the region where $\sigma(e^+e^- \rightarrow W^+W^-)$ is most sensitive to M_W . We found, by Monte Carlo simulation, that a simultaneous fit to both M_W and Γ_W resulted in a degraded value of M_W , while failing to provide a more precise value for Γ_W than that which is already known.

If the Standard Model is assumed to be correct, it is possible to calculate Γ_W with very little theoretical uncertainty. Unfortunately, we cannot use this calculated value in a measurement of M_W : It is, after all, equally possible to calculate M_W in the context of the Standard Model, and it would be inconsistent to let M_W vary while using the predicted value of Γ_W . This inconsistency manifests itself even if Γ_W is computed as a function of M_W : Depending on the method of calculation, it scales either as M_W^3 or as M_W^1 .

We will, then, simply use the measured value of Γ_W in our calculation; the uncertainty in this value will yield a systematic error in the measurement of M_W . Fortunately, the insensitivity of the W^+W^- cross section means that this error is small. Performing a numerical calculation to be described below, and using $\Gamma_W = 2.12 \pm 0.11$ GeV, we obtain $\delta M_W \approx 20$ MeV

Other sources of systematic error include uncertainty in the luminosity and in the calibration of the beam energy. From experiences at LEP 100, it is expected that the luminosity will be known to better than 1% [12] and that the beam energy will be known to within 20 MeV. Uncertainty in the luminosity affects the overall normalization, while, since we are essentially measuring the location of the threshold, an error in the energy calibration directly corresponds to an error in M_W .

Finally, performing this measurement requires knowing the efficiency for detecting and identifying a W^+W^- pair produced nearly at rest. There are two separate issues: The probability for misidentifying a W^+W^- event as something else, and the probability for incorrectly identifying some other type of event as a W^+W^- event. Events where at least one W decays to a charged lepton and a neutrino are probably distinctive enough that

misidentification is unlikely, but events where the final state consists of four jets must be considered more carefully.

For our purposes, what is important is not the absolute magnitude of these probabilities, but rather the uncertainty with which they are known. This uncertainty, which we denote $\Delta\epsilon$, takes the form of an additional uncertainty in the overall normalization of the measured cross section. The parameter $\Delta\epsilon$ can be determined only by detailed detector studies, but it is likely that it will be at most a few percent. Depending on its magnitude, this could be the dominant source of systematic error.

We summarize the various sources of systematic and theoretical error in Table II.

D. Realistic estimate of expected precision

We use a fitting procedure to estimate the statistical and systematic error more precisely: We simulate an experimental run by choosing the energies at which measurements will be made, and the luminosity that will be devoted to each measurement. Using Poisson statistics, we then randomly generate the number of W^+W^- events observed at each of these points. Finally, we perform a numerical fit of the W^+W^- cross section to these randomly generated measurements, taking M_W to be a free parameter; an example of such a fit is shown in Fig. 6. We can simulate systematic errors by using a different value of Γ_W or of the normalization constant when generating the numbers of events than when fitting the cross section.

The systematic and statistical errors are obtained directly by carrying out this procedure many times: The mean of the difference between the fitted value of M_W and the true value is the systematic error, while the variance is the statistical error. The different systematic errors are added in quadrature.

We find that, for integrated luminosities between 50 pb^{-1} and 1000 pb^{-1} , and for any reasonable assumptions about errors in Γ_W and in the cross section's normalization, the optimum strategy is to measure the cross section near threshold, *i.e.*, between 80 and 81 GeV. Assuming an integrated luminosity of 100 pb^{-1} , Fig. 7 shows the statistical error in M_W as a function of the energy at which the cross section is measured; note that the measurement rapidly becomes ineffective as the energy is raised much above threshold.

The systematic error due to uncertainty in the luminosity and the overall normalization of the cross section could be reduced by making additional measurements further above threshold, but this systematic error is already less than 50 MeV, which is sufficiently small that such an improvement would be negated by the increase in the statistical error that would result from lowering the statistics in the region of greatest sensitivity to M_W .

We use the values discussed in Sections III B and III C to estimate the systematic error. Adding the statistical and systematic error in quadrature yields the total error in measuring M_W , as a function of integrated luminosity; this is plotted in Fig. 8. Until very high luminosities are obtained, the measurement is dominated by statistics. Assuming an integrated luminosity of 100 pb^{-1} , we estimate that the total uncertainty will be about 100 MeV.

IV. CONCLUSION

Several methods have been proposed for measuring M_W to higher precision than is currently available; one of the most promising methods is to measure the threshold dependence of the total cross section for W^+W^- pair production at an e^+e^- collider.

There is, of course, some tension between this measurement and other physics goals of LEP 200: This measurement requires prolonged running in an energy region where the W^+W^- cross section is only a few picobarns, while many other measurements are best made at an energy as close as possible to the peak W^+W^- cross section. If it is possible to obtain an equally good measurement of M_W from reconstruction of hadronic W decays, that method may, at least initially, be preferable.

For these purposes, an elaborate calculation of this cross section is unnecessary: A modified tree level calculation includes most of the important physical effects, and is sufficiently precise to be compared to the measured cross section for the extraction of M_W . We have performed such a calculation, and, using these results, we estimate that with an integrated luminosity of 100 pb^{-1} it should be possible to measure M_W to a precision of about 100 MeV.

ACKNOWLEDGMENTS

This work was supported by the Director, Office of Energy Research, Office of High Energy and Nuclear Physics, Division of High Energy Physics of the U.S. Department of Energy under Contract DE-AC03-76SF00098.

APPENDIX: PARTICLES OF FINITE WIDTH IN THE FINAL STATE

If an unstable particle appears in the final state of a process, the naïve prescription for the cross section is to calculate the cross section for the particle to be produced with mass \sqrt{s} , and then convolve this result with some weighting function $\rho(s)$ that resembles a Breit-Wigner. In this Appendix, we derive a more precise form of this prescription, making manifest the approximations that are necessary for the derivation. We will derive a form for a final state containing a single W ; the generalization to two or more unstable particles is trivial.

The process that actually takes place is the emission of a virtual W , where the final-state particles are leptons and hadrons. If box diagrams can be neglected, this process can be factorized into the production of a W and its decay, *i.e.*,

$$\mathcal{M} = P_\mu \Delta^{\mu\nu} \mathcal{J}_\nu, \tag{A1}$$

where P^μ is the part of the amplitude dealing with W production and with any other particles in the process, $\Delta^{\mu\nu}$ is the W propagator, and \mathcal{J}_ν is the part dealing with W decay. Since box diagrams are nonresonant, neglecting them is an excellent approximation.

Phase space factorizes as well: we can write

$$d\Phi = d\Phi(p, q_1, \dots, q_m) d\Phi_W(k_1, \dots, k_n) (2\pi)^3 ds, \tag{A2}$$

where q_i are the momenta of the final-state particles other than the W , k_i are the momenta of the W 's decay products, p is the momentum of the W , and $s = p^2$. The cross section, then, may be written

$$d\sigma = A_{\mu\nu} W^{\mu\nu}, \quad (\text{A3})$$

where $W^{\mu\nu}$ comes from the W propagator and the W 's decay, and $A_{\mu\nu}$ is everything else.

By definition, calculating the cross section for production of a W means that we aren't interested in the details of what the W decays into, so we sum over all decay channels for the W and, for each channel, integrate over the phase space of the decay products. We will deal with a single decay channel; the sum over channels presents no additional complications. The result, then, is

$$\begin{aligned} W^{\mu\nu} &= (2\pi)^3 \int ds \Delta^{*\mu\alpha} \Delta^{\nu\beta} \int d\Phi_W(k_1, \dots, k_n) \mathcal{J}^\dagger_\alpha \mathcal{J}_\beta \\ &= (2\pi)^3 \int ds \Delta^{*\mu\alpha} \Delta^{\nu\beta} T_{\alpha\beta}, \end{aligned} \quad (\text{A4})$$

where

$$T_{\mu\nu} \equiv \int d\Phi_W(k_1, \dots, k_n) \mathcal{J}^\dagger_\mu \mathcal{J}_\nu. \quad (\text{A5})$$

It is always possible, of course, to write the integrand in Eq. (A4) as a product, and thus to write the cross section in the form

$$\sigma = \int ds \rho(s) \sigma_0(s). \quad (\text{A6})$$

This statement, by itself, has no physical content; the real content of Eq. (2) is that it is possible to define these functions in such a way that ρ can be interpreted as a Breit-Wigner and σ_0 can be interpreted as the cross section for production of a W with an unphysical value of the mass. It is important to remember, however, that σ_0 is not, in fact, the cross section for any physical process, and that its meaning must be defined by explicit construction.

We will define σ_0 to be the cross section for the production of a W that has an unphysical mass but that is still on-shell—that is, that still only has three polarization states. Consider, then, the amplitude for the decay of such an on-shell W with momentum p and mass \sqrt{s} . This W is an ordinary vector particle, so the amplitude is

$$\mathcal{M} = \epsilon_\mu^*(\sqrt{s}, p, \lambda) \mathcal{J}^\mu, \quad (\text{A7})$$

where ϵ is the W 's helicity vector, λ is the helicity index, and \mathcal{J} has the same meaning as before. Averaging over initial helicities,

$$d\Gamma(s) = \frac{(2\pi)^4}{2\sqrt{s}} d\Phi_W \cdot \frac{1}{3} \frac{1}{s} (p^\mu p^\nu - s g^{\mu\nu}) \mathcal{J}^\dagger_\mu \mathcal{J}_\nu, \quad (\text{A8})$$

where we have used the fact that

$$\sum_\lambda \epsilon_\mu^*(\sqrt{s}, p, \lambda) \epsilon_\nu(\sqrt{s}, p, \lambda) = \frac{1}{s} (p_\mu p_\nu - s g_{\mu\nu}). \quad (\text{A9})$$

Performing the phase space integral,

$$\Gamma(s) = \frac{(2\pi)^4}{2\sqrt{s}} \frac{1}{3} \frac{1}{s} (p^\mu p^\nu - s g^{\mu\nu}) T_{\mu\nu}. \quad (\text{A10})$$

If the masses of all fermions in the final state may be neglected, then the W couples to a conserved current, and we may write

$$T^{\mu\nu} = (p^\mu p^\nu - s g^{\mu\nu}) T(s). \quad (\text{A11})$$

In the case at hand this approximation is permissible: The heaviest fermion that a W can decay to is the b quark, and $m_b^2/M_W^2 < 0.004$. Eq. (A10) thus simplifies to

$$\Gamma(s) = (2\pi)^4 \sqrt{s} \frac{T(s)}{2}. \quad (\text{A12})$$

Note, however, that this simplifying approximation is crucial: If the masses of particles in the final states cannot be neglected, then no such simple form as Eq. (2) exists.

Similarly, returning to $W^{\mu\nu}$, Eq. (A4) simplifies as well. The gauge-dependent piece of the W propagator vanishes when contracted with a tensor of the form given in Eq. (A11), so we may write

$$\Delta^{\mu\nu} = \Delta(s) g^{\mu\nu}, \quad (\text{A13})$$

and, using Eq. (A12),

$$W_{\mu\nu} = \int ds |\Delta(s)|^2 \frac{\sqrt{s}\Gamma(s)}{\pi} \sum_\lambda \epsilon_\mu^*(\sqrt{s}, p, \lambda) \epsilon_\nu(\sqrt{s}, p, \lambda). \quad (\text{A14})$$

The $W_{\mu\nu}$ tensor is the only part of the cross section that depends on the details of the W in the final state, and this sum over the product of polarization vectors is the form that $W_{\mu\nu}$ would have if the final-state particle were a W of mass \sqrt{s} , so we have established that

$$\sigma = \int ds |\Delta(s)|^2 \frac{\sqrt{s}\Gamma(s)}{\pi} \sigma_0(s). \quad (\text{A15})$$

Now consider the form of $\Delta(s)$. At tree level,

$$\Delta(s) = \frac{-i}{s - M_W^2 + i\epsilon}, \quad (\text{A16})$$

but, including the vacuum polarization of the W , it becomes

$$\Delta(s) = \frac{-i}{s - M_W^2 + \delta M_W^2 - \Pi_{WW}(s)}. \quad (\text{A17})$$

If M_W is taken to be the physical W mass, then $\text{Re} \Pi_{WW}(M_W^2)$ exactly cancels the W mass counterterm δM_W^2 , so

$$\Delta(s) = \frac{-i}{s - M_W^2 - i\text{Im} \Pi_{WW}(s) - \text{Re} \tilde{\Pi}_{WW}(s)}, \quad (\text{A18})$$

where $\tilde{\Pi}(s) \equiv \Pi(s) - \Pi(M_W^2)$. We are only interested in $s \approx M_W^2$, and $\text{Re } \tilde{\Pi}(s)$ is a smooth function of s that, by construction, vanishes at $s = M_W^2$. It can thus be absorbed into the wave-function renormalization, and we neglect it as a non-leading correction.

Using the optical theorem, we can show [8] that

$$- \text{Im } \Pi_{WW}(s) = \sqrt{s}\Gamma(s), \quad (\text{A19})$$

where $\Gamma(s)$ is the decay rate for an on-shell W of mass \sqrt{s} . Finally, then, we can evaluate $\Gamma(s)$ either by performing the tree-level calculation, or by scaling the measured value. We choose the latter method. If the W 's decay products are massless, then $\Gamma(s)$ scales as \sqrt{s} , so

$$\Gamma(s) = \sqrt{s} \frac{\Gamma}{M_W}, \quad (\text{A20})$$

where Γ is the measured width of the physical W .

Substituting into Eq. (A15), we obtain

$$\sigma = \int ds \frac{1}{(s - M_W^2)^2 + s\Gamma^2(s)} \frac{\sqrt{s}\Gamma(s)}{\pi} \sigma_0(s) \quad (\text{A21})$$

$$= \int ds \frac{1}{(s - M_W^2)^2 + s^2\Gamma^2/M_W^2} \frac{s\Gamma}{\pi M_W} \sigma_0(s), \quad (\text{A22})$$

thus verifying Eq. (2).

REFERENCES

- [1] Particle Data Group, M. Aguilar-Benitez et al., Phys. Rev. **D45**, Part 2 (1992).
- [2] G. P. Yeh, "CDF: Recent Results and Future Prospects," FERMILAB-Conf-92/76/E, 1992 (unpublished).
- [3] D. Treille, Beam Line, Fall 1992, p. 17.
- [4] T. Muta, R. Najima, and S. Wakaizumi, Mod. Phys. Lett. **A1**, 203 (1986).
- [5] O. P. Sushkov, V. V. Flambaum, and I. B. Khriplovich, Sov. J. Nucl. Phys. **20**, 537 (1975). W. Alles, C. Boyer, and A. J. Buras, Nucl. Phys. **B119**, 125 (1977).
- [6] U. Amaldi, W. de Boer, and H. Fürstenau, Phys. Lett. **B260**, 447 (1991).
- [7] E. A. Kuraev and V. S. Fadin, Yad. Fiz. **41**, 733 (1985).
- [8] R. N. Cahn, Phys. Rev. **D36**, 2666 (1987).
- [9] M. Lemoine, M. Veltman, Nucl. Phys. B164, 445 (1980). R. Philippe, Phys. Rev. **D26**, 1588 (1982). M. Böhm et al., Nucl. Phys. **B304**, 463 (1988). J. Fleischer, K. Kolodziej, F. Jegerlehner, Phys. Rev. **D47**, 830 (1993).
- [10] K. Hagiwara and D. Zeppenfeld, Phys. Lett. **B196**, 1 (1987). B. Grzadkowski, Z. Hioki, and J. H. Kühn, Phys. Lett. **B205**, 388 (1988).
- [11] See, for example, R. N. Cahn, "Z decays and tests of the Standard Model," Proceedings of the 18th Annual SLAC Summer Institute on Particle Physics, 1990.
- [12] D. Treille, private communication, 1993.

TABLES

TABLE I. W^+W^- pair production cross section, including the finite value of Γ_W and the effects of initial-state radiation, for seven values of the W mass. The present value is $M_W = 80.22 \pm 0.26$ GeV. The cross section is a smooth function of M_W , and linear interpolation should suffice for values of M_W in between those presented here.

\sqrt{s} (GeV)	σ (pb)						
	79.6 GeV	79.8 GeV	80.0 GeV	80.2 GeV	80.4 GeV	80.6 GeV	80.8 GeV
150	0.447	0.424	0.402	0.382	0.363	0.346	0.329
151	0.508	0.480	0.454	0.430	0.408	0.387	0.368
152	0.582	0.547	0.516	0.487	0.461	0.436	0.413
153	0.675	0.632	0.593	0.557	0.525	0.495	0.468
154	0.793	0.738	0.689	0.644	0.604	0.567	0.534
155	0.951	0.877	0.812	0.755	0.704	0.657	0.616
156	1.169	1.067	0.978	0.901	0.832	0.772	0.719
157	1.485	1.336	1.209	1.100	1.007	0.925	0.854
158	1.965	1.738	1.547	1.387	1.252	1.137	1.038
159	2.689	2.353	2.064	1.820	1.615	1.443	1.298
160	3.651	3.225	2.831	2.478	2.170	1.908	1.688
161	4.704	4.256	3.812	3.383	2.978	2.609	2.284
162	5.728	5.293	4.853	4.410	3.971	3.540	3.129
163	6.676	6.268	5.851	5.427	4.996	4.561	4.128
164	7.539	7.159	6.771	6.373	5.968	5.554	5.133
165	8.324	7.970	7.608	7.238	6.860	6.473	6.078
166	9.038	8.707	8.369	8.024	7.672	7.311	6.943
167	9.689	9.378	9.061	8.744	8.409	8.073	7.730
168	10.284	9.992	9.694	9.391	9.082	8.767	8.446
169	10.830	10.552	10.272	9.987	9.696	9.400	9.099
170	11.330	11.068	10.803	10.533	10.257	9.979	9.696
171	11.789	11.541	11.289	11.034	10.774	10.510	10.241
172	12.212	11.976	11.736	11.494	11.247	10.997	10.744
173	12.601	12.376	12.148	11.917	11.683	11.445	11.204
174	12.961	12.746	12.528	12.307	12.084	11.858	11.629
175	13.294	13.088	12.878	12.668	12.454	12.238	12.020
176	13.601	13.403	13.203	13.001	12.797	12.590	12.381
177	13.885	13.695	13.503	13.309	13.113	12.915	12.715
178	14.148	13.965	13.781	13.595	13.406	13.216	13.024
179	14.391	14.215	14.037	13.858	13.678	13.495	13.310
180	14.616	14.446	14.275	14.102	13.928	13.752	13.575
181	14.824	14.660	14.495	14.328	14.160	13.991	13.820
182	15.016	14.857	14.698	14.537	14.375	14.212	14.047
183	15.193	15.040	14.886	14.730	14.574	14.416	14.257
184	15.357	15.209	15.060	14.909	14.758	14.605	14.451
185	15.508	15.365	15.220	15.075	14.928	14.780	14.631
186	15.648	15.508	15.368	15.227	15.085	14.942	14.798
187	15.776	15.641	15.505	15.368	15.230	15.091	14.952
188	15.894	15.767	15.630	15.497	15.364	15.229	15.093
189	16.002	15.875	15.746	15.621	15.487	15.356	15.225
190	16.102	15.977	15.852	15.727	15.600	15.477	15.345

TABLE II. Sources of systematic error in the measurement of M_W by study of the threshold, as discussed in Sections III C and III D; errors are added in quadrature. Many of these errors take the form of uncertainty in the overall normalization, which allows us to use Eq. (21). We are unable to estimate the uncertainty in detection efficiency, so we parameterize it as $\Delta\epsilon$. In our plots, we assume $\Delta\epsilon = 2\%$. All of these errors are sufficiently small that the measurement will be dominated by statistical error.

Effect	Effect on normalization	Error in M_W
Coupling constants	negligible	negligible
Model dependence	negligible	negligible
One-loop corrections	1%	17 MeV
Initial-state radiation	1%	17 MeV
Smearing approximation	negligible	negligible
Total theoretical error	1.5%	20 MeV
Γ_W		20 MeV
Luminosity	1%	17 MeV
Beam energy		20 MeV
Detection efficiency	$\Delta\epsilon$	$(17 \text{ MeV}) \times \Delta\epsilon$
Total systematic error		45 MeV

FIGURES

FIG. 1. Tree-level Feynman diagrams for W^+W^- pair production at an e^+e^- collider. Exchange of a virtual Higgs boson also contributes, but is negligible.

FIG. 2. Comparison of an exact tree-level calculation of $\sigma(e^+e^- \rightarrow W^+W^-)$, in which both W 's in the final state are integrated over Breit-Wigners, to an approximate calculation, in which only one W is integrated over a Breit-Wigner, but using a width twice the physical value. Note that this is an excellent approximation except in a domain so far below threshold that the cross section is unobservably small. The peak at 45 GeV is due to the decay of a Z to two virtual W 's.

FIG. 3. Calculation of $\sigma(e^+e^- \rightarrow W^+W^-)$. The solid curve is the tree-level cross section where both final-state W 's are on-shell, the dashed curve is the cross section where the W 's are allowed to be off-shell, and the dotted curve includes initial-state radiation as well as the finite W width. Note that the finite width of the W and the initial-state radiation are effects of comparable magnitude.

FIG. 4. Calculation of $\sigma(e^+e^- \rightarrow W^+W^-)$, including the finite width of the W and the effect of initial-state radiation. The solid curve is for $M_W = 80.0$ GeV, the dashed curve is for $M_W = 80.2$ GeV, and the dotted curve is for $M_W = 80.4$ GeV. The dependence on M_W is strongest for $E \approx M_W$.

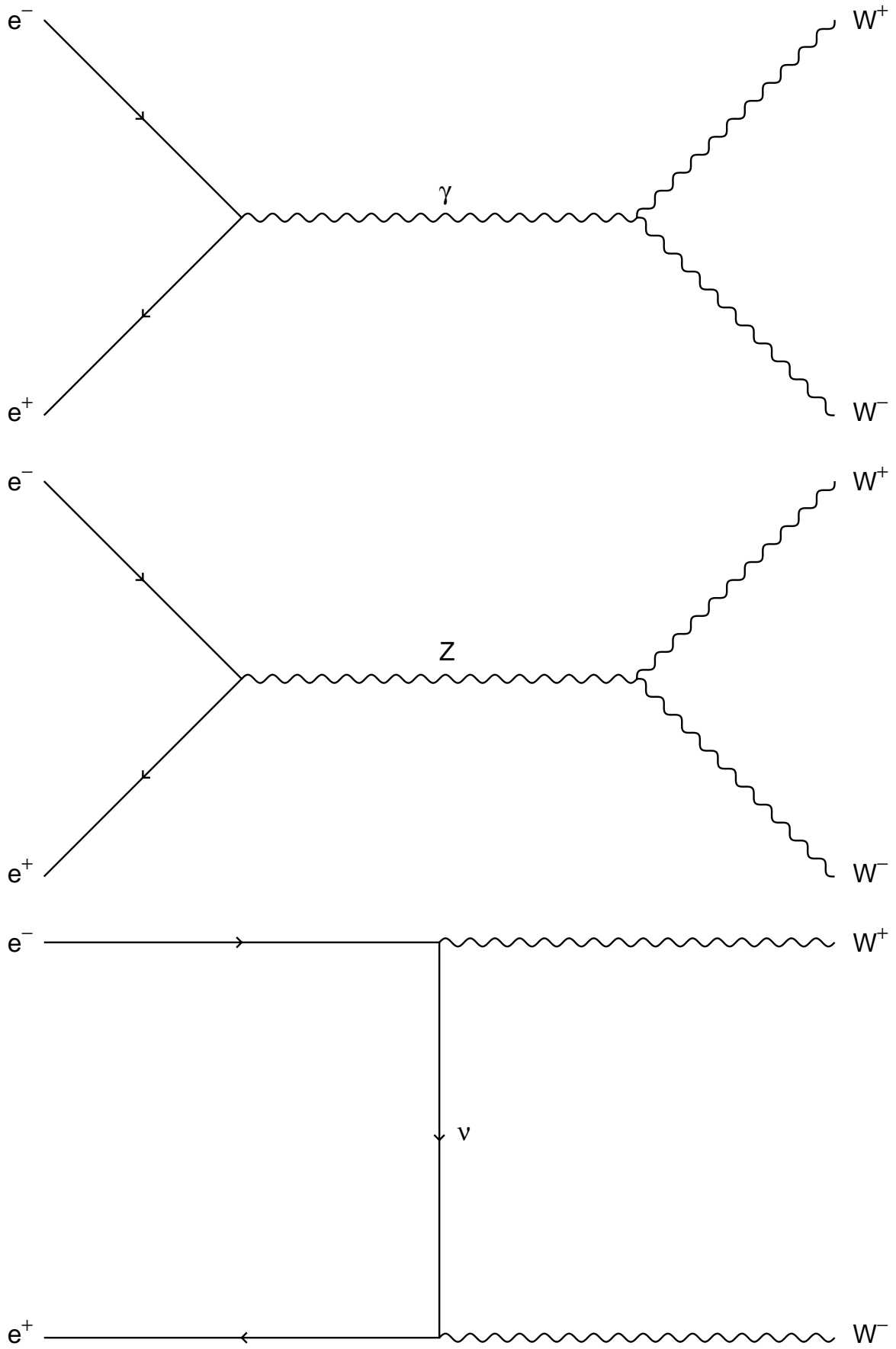
FIG. 5. Calculation of $\sigma(e^+e^- \rightarrow W^+W^-)$, including the finite width of the W and the effect of initial-state radiation. The three curves represent different values for Γ_W : the solid curve is with $\Gamma_W = 1.9$ GeV, the dashed curve is with $\Gamma_W = 2.1$ GeV, and the dotted curve is with $\Gamma_W = 2.3$ GeV. The measured value is $\Gamma_W = 2.12 \pm 0.11$ GeV. Note that for values of the width close to the measured value, the form of the cross section is not very sensitive to Γ_W .

FIG. 6. Simulation of an experimental determination of M_W , using an integrated luminosity of 100pb^{-1} . Measurements are made at 80.1 GeV, 80.5 GeV, and 80.9 GeV. At each point, the number of observed events is randomly chosen, using a Poisson distribution whose mean is the cross section times the integrated luminosity. The points, with $1\text{-}\sigma$ error bars, represent these simulated measurements of σ at those three energies, and the solid curve, which corresponds to $M_W = 80.31$ GeV, is the best fit.

FIG. 7. Statistical error in the measurement of M_W , in MeV, as a function of the energy at which $\sigma(e^+e^- \rightarrow W^+W^-)$ is measured. Note that the statistical error is quite high unless the measurement is made at the W^+W^- threshold. This plot is generated assuming an integrated luminosity of 100pb^{-1} , but this qualitative feature is true independent of luminosity. The total cross section at this energy is roughly 0.3 pb, compared to a peak value of more than 16 pb.

FIG. 8. Estimated error in the measurement of M_W , in MeV, as a function of integrated luminosity. The solid curve is the total error, and the dotted curve is the statistical error. Note that until very high luminosities are obtained, the measurement is dominated by statistical error.

Figure 1



$$\sigma(e^+ e^- \rightarrow W^+ W^-)$$

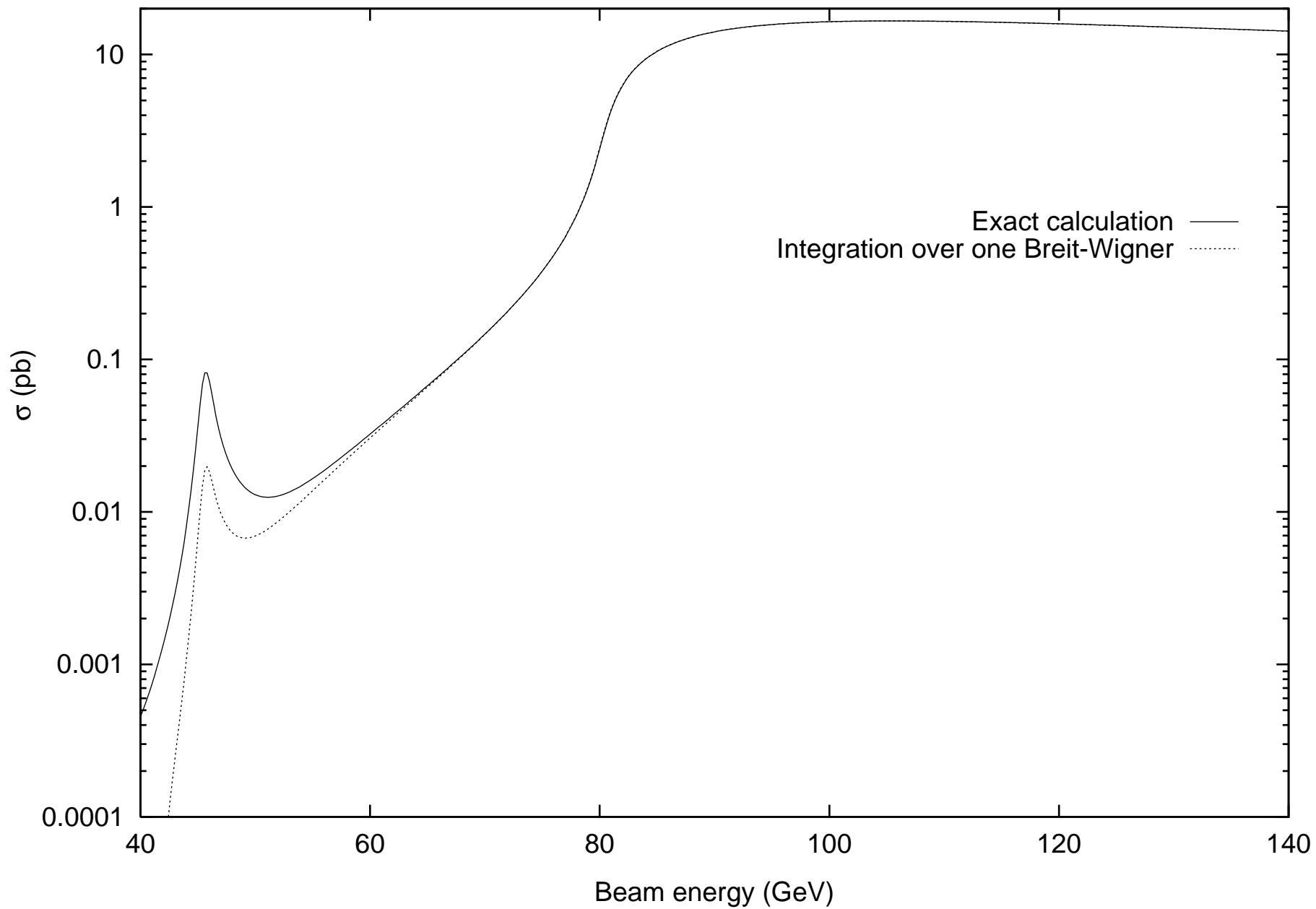


Figure 2

Cross section for $e^+ e^- \rightarrow W^+ W^-$

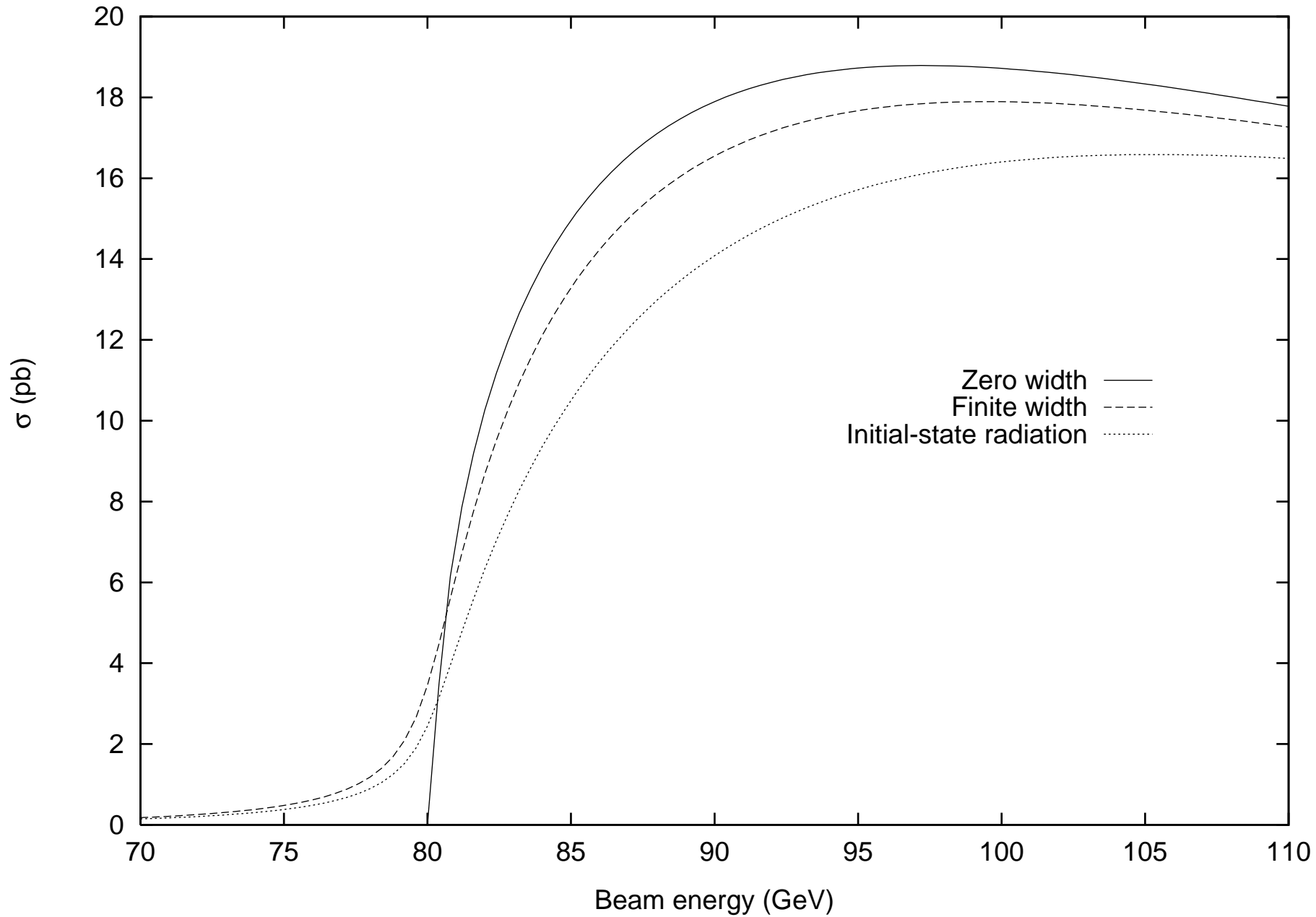


Figure 3

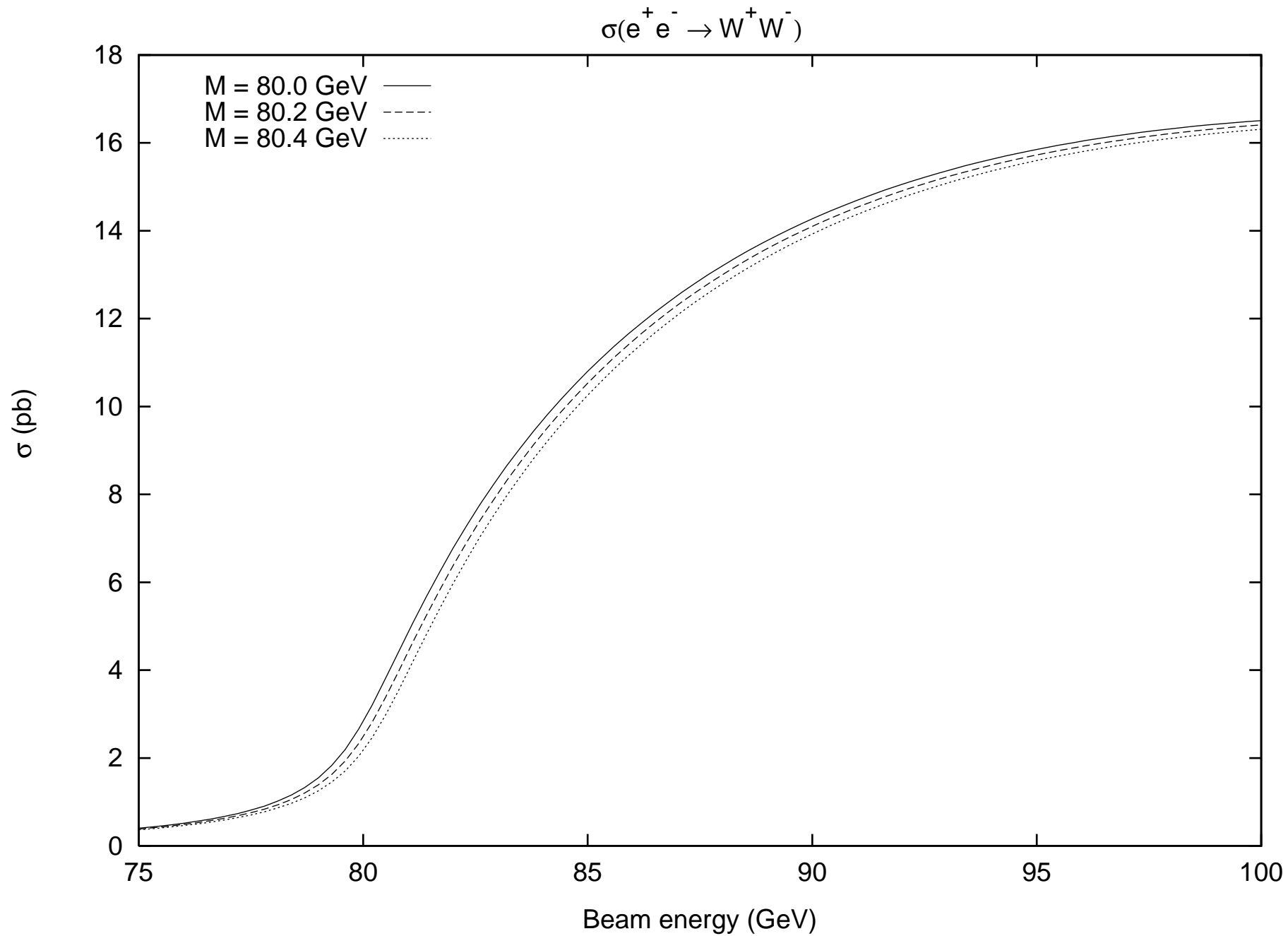


Figure 4

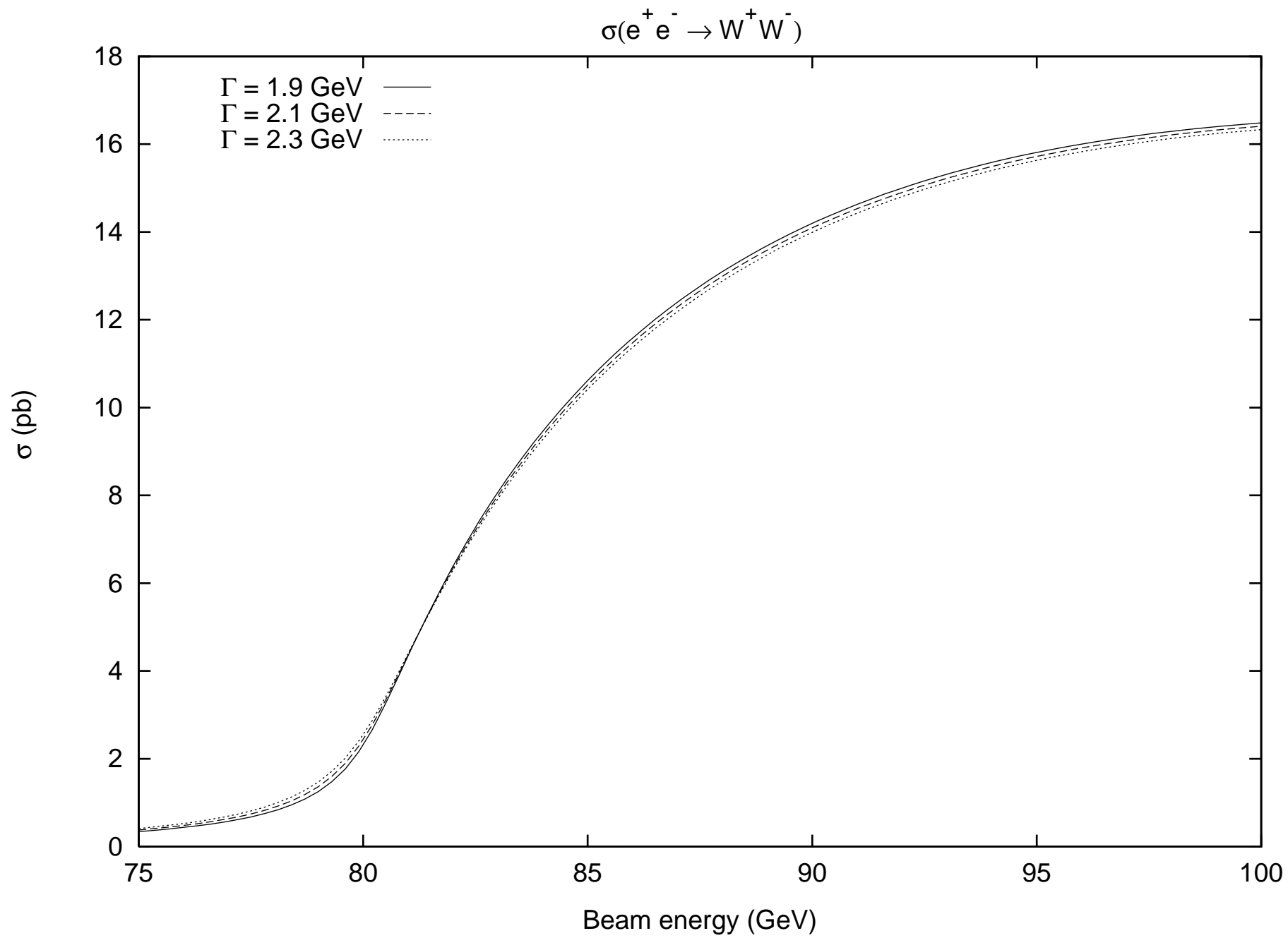


Figure 5

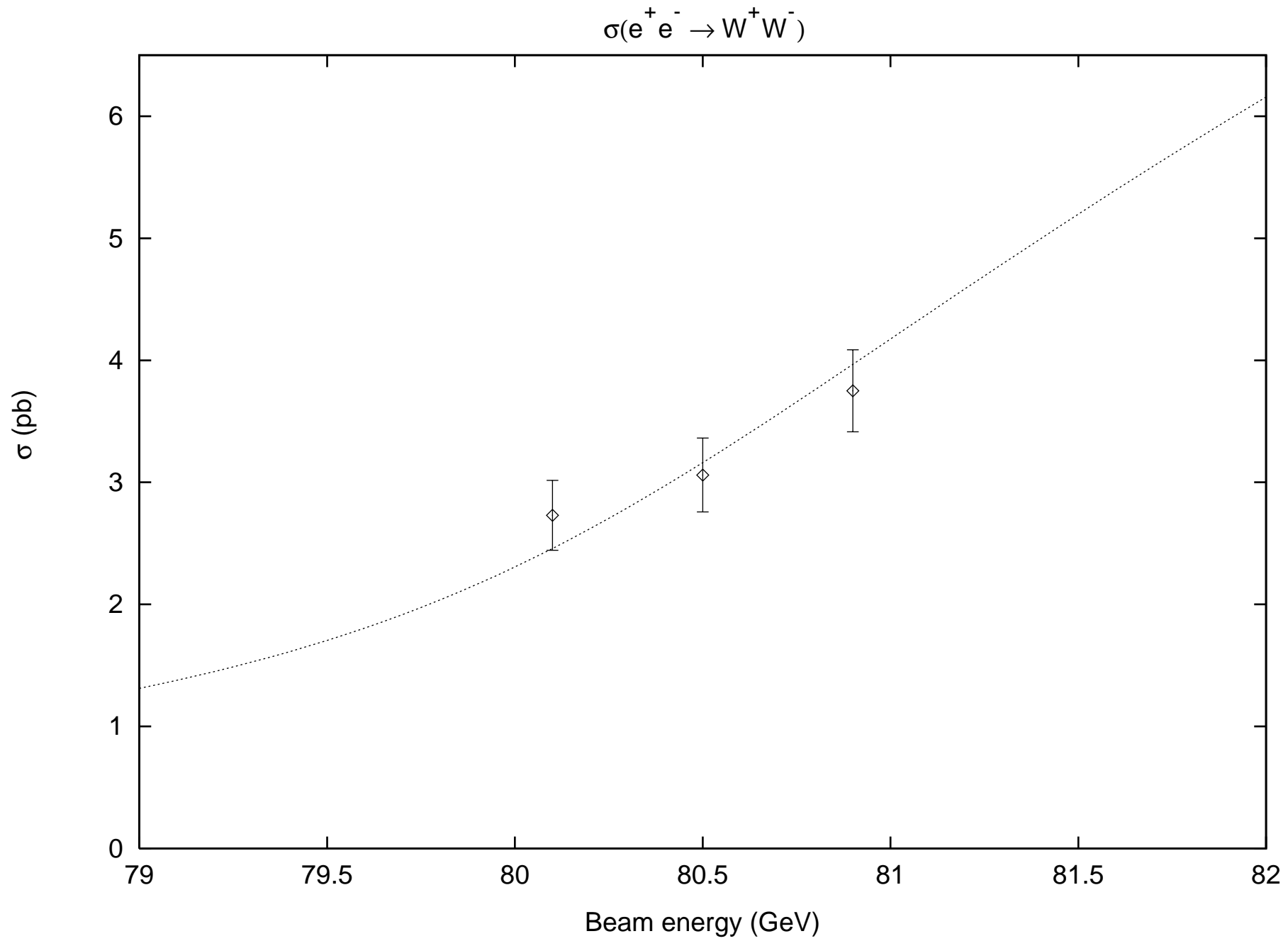


Figure 6

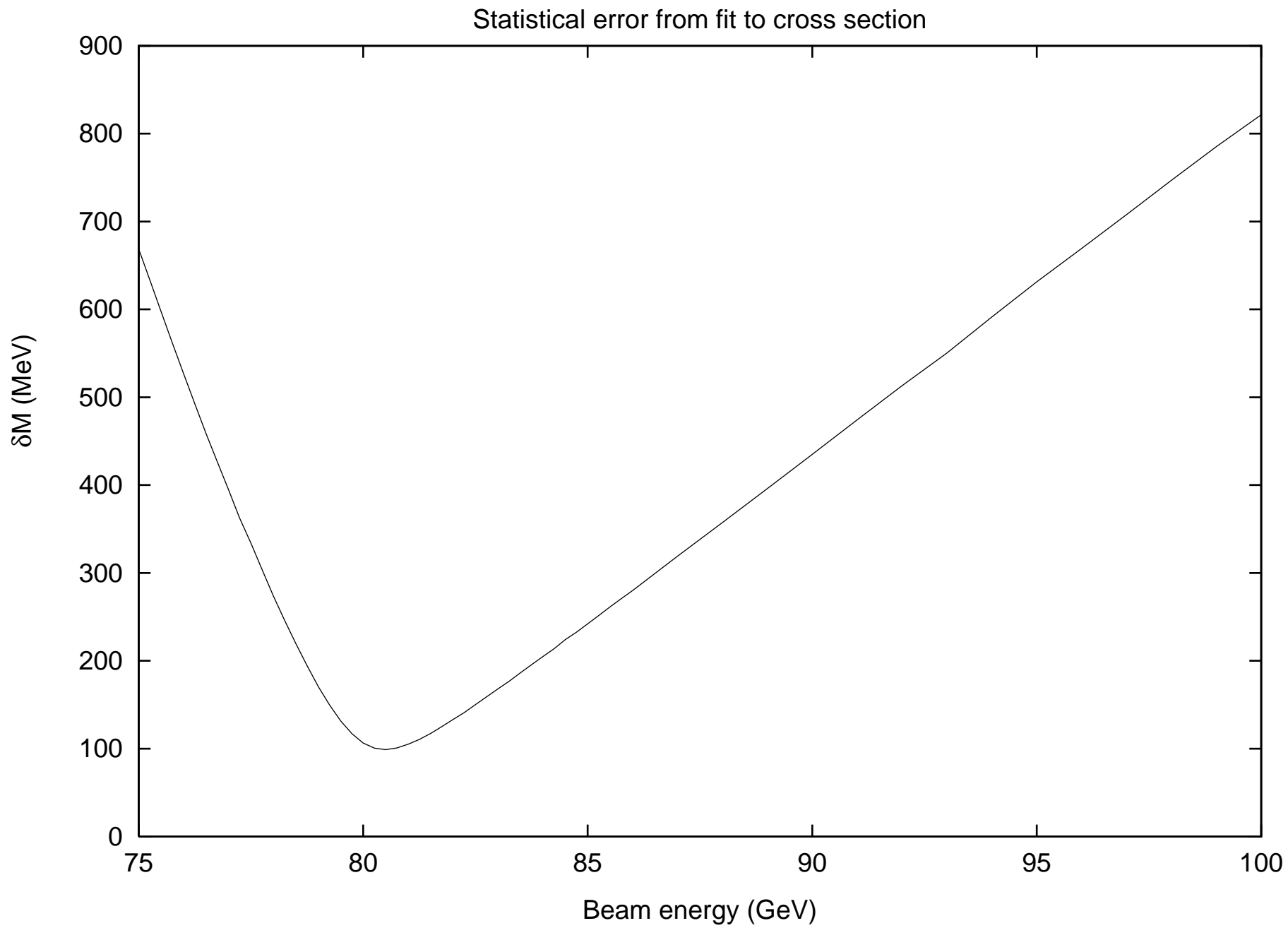


Figure 7

Precision of mass measurement

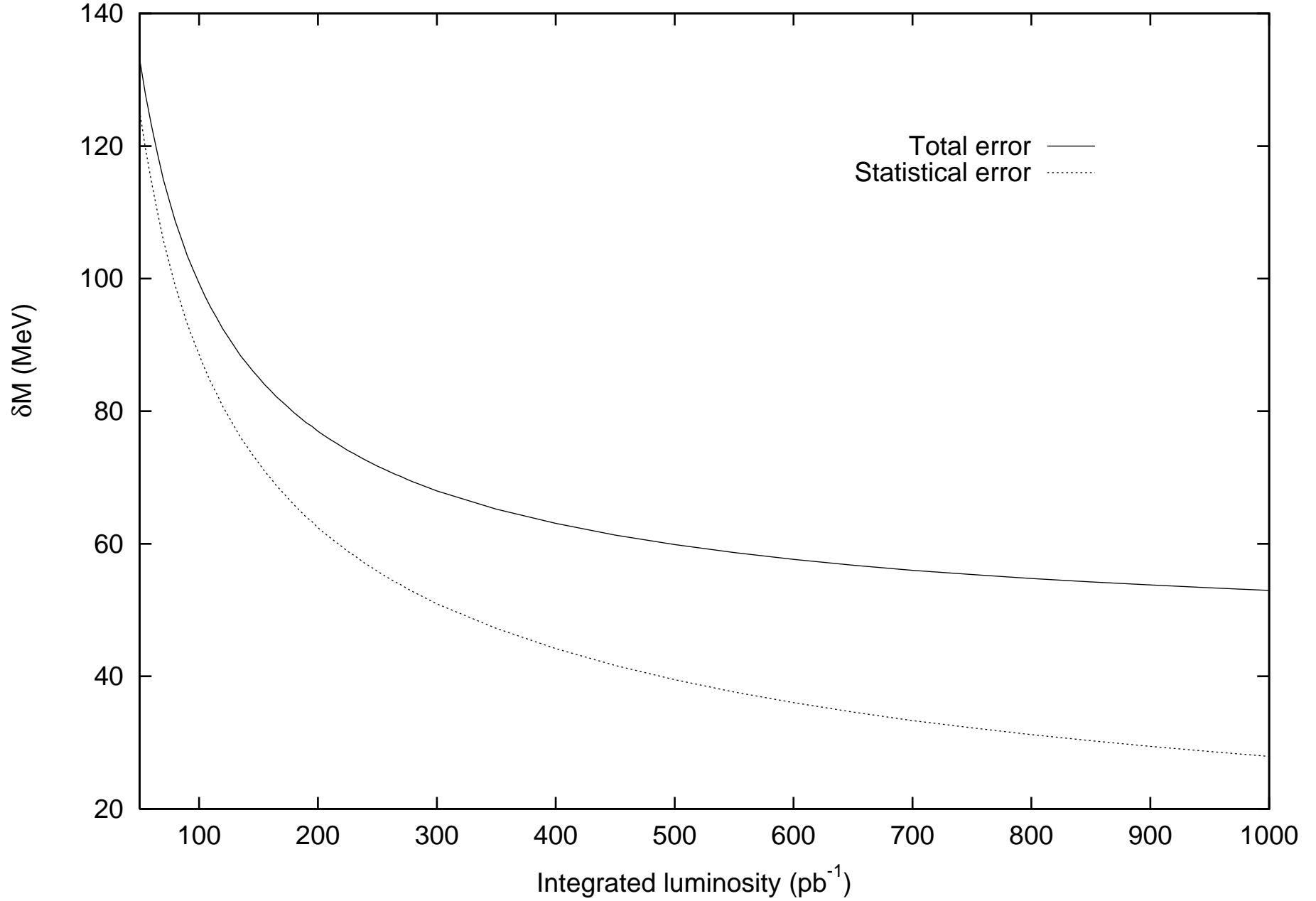


Figure 8